

Article

Green Synthesis of Silver Nanoparticles Using *Juniperus procera* Extract: Their Characterization, and Biological Activity

Merajuddin Khan ^{1,*}, Ponmurugan Karuppiyah ², Hamad Z. Alkhatlan ¹, Mufsir Kuniyil ¹,
Mujeeb Khan ^{1,*}, Syed Farooq Adil ¹ and Mohammed Rafi Shaik ^{1,*}

¹ Department of Chemistry, College of Science, King Saud University, P.O. Box 2455, Riyadh 11451, Saudi Arabia; khathlan@ksu.edu.sa (H.Z.A.); mkuniyil@ksu.edu.sa (M.K.); sfadil@ksu.edu.sa (S.F.A.)

² Department of Botany and Microbiology, College of Science, King Saud University, P.O. Box 2455, Riyadh 11451, Saudi Arabia; pkaruppiyah@ksu.edu.sa

* Correspondence: mkhan3@ksu.edu.sa (M.K.); kmujeeb@ksu.edu.sa (M.K.); mrshaik@ksu.edu.sa (M.R.S.); Tel.: +966-11-4670439 (M.R.S.)

Abstract: Plant extract-based green synthesis of metal nanoparticles (NPs) has become a popular approach in the field of nanotechnology. In this present investigation, silver nanoparticles were prepared by an efficient and facile approach using *Juniperus procera* extract as a bioreducing and stabilizing agent. The as-synthesized silver nanoparticles (JP-AgNPs) were characterized by several characterization techniques such as UV-Vis, XRD, FT-IR, HR-TEM, and EDX analysis. The XRD analysis evidently confirms that the as-synthesized Ag nanoparticles (NPs) from *Juniperus procera* plant extract (JP-AgNPs) are crystalline in nature. FT-IR analysis confirms that the plant extract plays a dual role as a bioreducing and capping agent, while HR-TEM revealed the spherical morphology of as-synthesized JP-AgNPs with the size of ~23 nm. Furthermore, the synthesized JP-AgNPs were evaluated for antibacterial properties against several bacterial and fungal strains such as *Staphylococcus aureus* (ATCC 12228), *Escherichia coli* (ATCC 25922), *Pseudomonas aeruginosa* (ATCC 27853), *Proteus mirabilis* (ATCC 4753), *Cryptococcus neoformans* (ATCC 16620), and *Candida albicans* (ATCC 885-653). The JP-AgNPs displayed an efficient mean zone of inhibition (MZI) at 50.00 μ L for bacterial associated with fungal pathogens than the plant extract. Mainly, MZI values against microbial pathogens were as follows; *E. coli* (17.17 \pm 0.72 mm), *P. mirabilis* (14.80 \pm 0.17 mm), and *C. albicans* (14.30 \pm 0.60 mm), whereas JP-AgNPs showed moderate activity against *P. aeruginosa* (11.50 \pm 0.29 mm) and *C. neoformans* (9.83 \pm 0.44 mm). Notably, the tested JP-AgNPs have displayed almost similar antimicrobial activities with that of standard antimicrobial drugs, such as streptomycin and nystatin. The enhanced antimicrobial activity of JP-AgNPs can be ascribed to the quality of resultant NPs including, uniform size, shape, and aqueous colloidal stability of nanoparticles.

Keywords: silver nanoparticle; natural products; *Juniperus procera* plant; green synthesis; biological activity



Citation: Khan, M.; Karuppiyah, P.; Alkhatlan, H.Z.; Kuniyil, M.; Khan, M.; Adil, S.F.; Shaik, M.R. Green Synthesis of Silver Nanoparticles Using *Juniperus procera* Extract: Their Characterization, and Biological Activity. *Crystals* **2022**, *12*, 420. <https://doi.org/10.3390/cryst12030420>

Academic Editor: Borislav Angelov

Received: 3 March 2022

Accepted: 16 March 2022

Published: 18 March 2022

Publisher's Note: MDPI stays neutral with regard to jurisdictional claims in published maps and institutional affiliations.



Copyright: © 2022 by the authors. Licensee MDPI, Basel, Switzerland. This article is an open access article distributed under the terms and conditions of the Creative Commons Attribution (CC BY) license (<https://creativecommons.org/licenses/by/4.0/>).

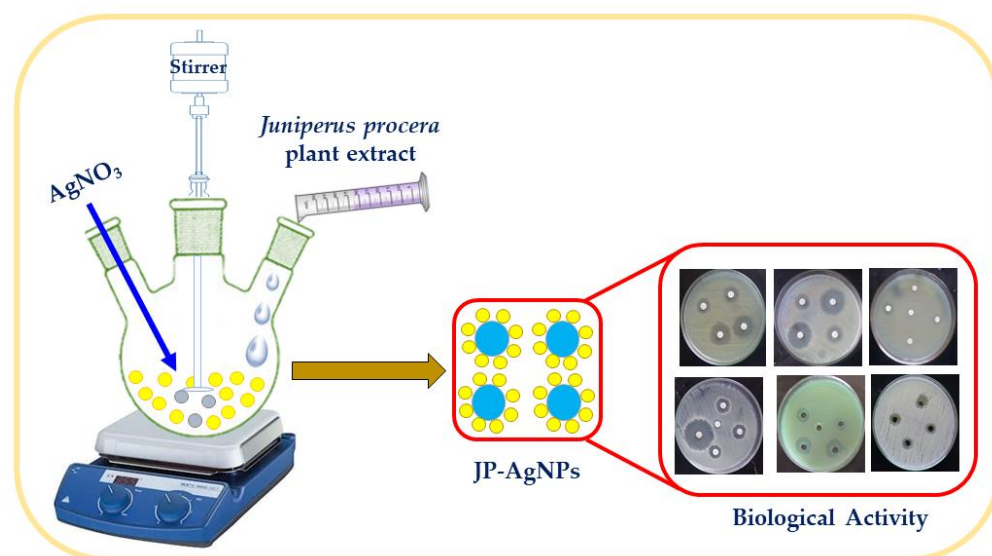
1. Introduction

Nanotechnology is a prominent field in material science [1], which effectively combines various disciplines of basic sciences including engineering [2], physics [3], chemistry [4], and biological sciences [5]. Principal to the advancement of this field is the development of novel approaches for the efficient and facile preparation of nanoparticles (NPs). NPs offer remarkable physico-chemical characteristics when compare to their bulk counterparts, which have been successfully utilized for various advanced applications [6]. So far, NPs have been produced through various approaches involving a variety of physical, chemical and biological processes. Generally, most of the physical, chemical and hybrid approaches are expensive and hazardous in nature due to the involvement of sophisticated instruments and toxic materials including solvents, reducing agents and precursors etc. [7]. On the other

hand, NPs preparation using green approaches is less expensive, eco-friendly and easy to apply. Hence, these approaches have become popular and are increasingly employed for the eco-friendly preparation of metallic NPs. To date, the green synthesis of NPs has been attempted using a variety of natural materials like microorganisms, biomolecules and plant extracts etc. [8]. Although a significant number of studies have been published in the literature on the green synthesis of NPs using biomolecules, microorganisms and plant extracts, plant extracts are more favored over other natural materials [7,9,10]. Since plant extract-based approaches are inexpensive, efficient, and does not involve a cumbersome process of the isolation of the biomolecules and storing the microbial cultures etc. [11]. Moreover, plants based synthesis of nanomaterials does not require expensive reagents, high temperatures and pressure etc.

Among various materials, NPs developed from noble metals have received significant recognition over the past few decades, as they can be utilized in sensors, biomedical devices and various other advanced applications [8,12–15]. Out of a variety of metallic NPs, silver NPs have received immense popularity owing to their extraordinary characteristics, comprising of excellent electrical conductivity, high chemical stability, and superior antibacterial activity [16]. Therefore, the synthesis of silver nanoparticles has been attempted using a number of methods and still is an evolving field. Chemically synthesized Ag NPs are of high quality, however, they are mostly not suitable for biomedical application due to the chances of contamination of resulting NPs with the hazardous chemical used during their synthesis. Since the biocompatibility of nanomaterials is of utmost importance when they are considered for biological applications. The green synthesis of Ag NPs using plant extracts is an attractive option, which is less likely to contaminate the final products. [17]. Due to this, several studies have demonstrated the successful preparation of Ag NPs using the extracts of various plants, such as *Origanum vulgare* L. [16], *Pulicaria glutinosa* [17], *Cordia myxa* [18], and *Salvadora persica* [7]. In addition to the whole plant extracts, other components of the plants like seeds, roots, leaves, fruits, and stems have been also been applied to prepare diverse metallic nanoparticles. Since these parts are known to contain a wide range of phytochemicals in their extracts, which can effectively play the role of stabilizing and bioreducing agents for the synthesis of nanoparticles [18,19]. In this context, *Juniperus procera* extract, which is known to consist of a variety of polyphenolic phytoconstituents will be a potential candidate to be explored for the preparation of NPs. However, this has been rarely investigated for the synthesis of silver nanoparticles. *Juniperus procera* plant belongs to the *Cupressaceae* family, and phytochemicals of this plant are known to possess excellent antioxidant, antimicrobial, and anticancer activities. Several literature reports stated that more than 65 species allied to *Juniperus* are spreading all over the world. Analyses performed on *J. procera* extracts revealed the occurrence of several constituents that might replicate its pharmacological properties [20]. Although *Juniperus procera* has been used prior for the preparation of Ag NPs, only its leaves' extract is known to produce NPs [21]. Besides, the resultant Ag NPs were not of very good quality due to the large size and wide size distribution of particles between 30–90 nm. To the best of our knowledge, the extract of the whole aerial parts of the plant has never been used for this purpose.

Herein, in the present study, a biosynthesis approach was adopted for the synthesis of silver nanoparticles using *J. procera* extract. The as-synthesized silver nanoparticles (JP-AgNPs) were characterized by several characterization techniques such as UV-Vis, XRD, FT-IR, TEM, and EDX analysis. Furthermore, the synthesized silver nanoparticles were investigated for biological activity using various bacterial and fungal strains (Scheme 1).



Scheme 1. Graphical representation of silver nanoparticles (JP-AgNPs) synthesis using *J. procera* extract.

2. Materials and Methods

2.1. Materials

The aerial parts of *J. procera* are abundantly available in the Al-Baha region of Saudi Arabia and were collected in the month of April-2020. After the collection of plant material it was firstly identified in the herbarium division by a plant taxonomist at King Saud University, Riyadh. A voucher specimen (HZKJP-20) of the *J. procera* is maintained with us. AgNO_3 (99.8%, Sigma Aldrich, St. Louis, MO, USA), and other chemicals and solvents exploited in this work were purchased from Sigma Aldrich.

2.2. Preparation of Plant Extract for the Synthesis of Ag NPs

To start with, fresh aerial parts of the *J. procera* were first dried at room temperature and ground into small pieces. About 1 kg of *J. procera* aerial parts was refluxed for ~3 h on a heating mantle at 80 °C. After three hours of reflux, the solution was allowed to cool down and filtered. The water extract obtained was dried completely on a rotary evaporator to get the dark brownish color extract. The resultant extract was stored at room temperature and was used for the synthesis of silver nanoparticles. 1.0 g extract from aerial parts of the *J. procera* was dissolved in 10 mL of DI water and was used for the NPs synthesis.

2.3. Preparation of Silver Nanoparticles Using *J. procera* (JP-AgNPs)

The synthesis of silver nanoparticles (JP-AgNPs) was carried out by adding 1 mL from the stock solution of the aerial part extract of the *J. procera* to 50 mL of 0.5 mM of AgNO_3 aqueous solution in a 250 mL flask. The flask with the resultant solution is attached with a magnetic stir bar and fixed on a condenser. The reaction was continued for ~120 min at 90 ± 5 °C. While stirring, the reaction color transformed from light green to dark brown color, and afterward, no further color transformation is perceived until the end of the reaction. To eliminate any prospect of the existence of unbound residual phytomolecules on the surface of the green as-synthesized JP-AgNPs, it is re-dispersed in double distilled water via sonication for 20 min after centrifugation, this procedure is continued three times to isolate pure JP-AgNPs. Afterward, the attained reaction product is washed three times with double distilled water, and then the obtained product was dried at 70 °C for 12 h in an oven. Finally, a black powder is achieved.

2.4. Preparation of Plant Extracts and JP-AgNPs for Biological Activity

Juniperus procera, sect. *Sabina* is commonly known as African-cedar. It is a coniferous tree native of Africa and the Arabian Peninsula. In order to prepare the samples for biologi-

cal studies, one milligram of extracted plant powder (JP) and one mg of biosynthesized silver nanoparticle (JP-AgNPs) were separately dissolved in one mL of dimethyl sulfoxide (DMSO) each. In this case, the final concentrations of both the samples remained 1 mg/mL.

2.5. Antimicrobial Activity of JP-AgNPs

The antibacterial and antifungal activity was performed as per method agar well diffusion method described by Bonev et al. (2008) [22]. Selected bacterial and fungal strains used in the antimicrobial assessment were procured from the Microbiology Lab, King Khalid University Hospital, Riyadh, Saudi Arabia. A list of microbial pathogens namely, *Staphylococcus aureus* (ATCC 12228), *Escherichia coli* (ATCC 25922), *Pseudomonas aeruginosa* (ATCC 27853), *Proteus mirabilis* (ATCC 4753), *Cryptococcus neoformans* (ATCC 16620), and *Candida albicans* (ATCC 885-653). Concisely, Sabouraud dextrose agar (SDA) for *C. albicans* and *C. neoformans* and Mueller-Hinton for bacterial strains was poured into Petri plates. The agar plates were swabbed with broth cultures standardized with 0.5 McFarland standard (1.0×10^8 CFU/mL). six mm well containing known concentrations of plant extract (JP), JP-AgNPs, and standard drug (10 µg) were loaded and then incubated at 37 °C for 24 h. Well loaded only with DMSO consider as a negative control. The streptomycin and nystatin were kept as positive controls for bacterial and fungal pathogens, respectively. The mean zone of inhibition (MZI) in millimeters (mm) was determined for each microbial pathogen in later incubation periods. All experiments were conducted in triplicate. The JP-AgNPs with MZI values more than or equal to 12.00 mm were selected for minimum inhibitory concentration (MIC) assays.

For MIC assay [23], a stock solution (mg/mL) of test JP-AgNPs was dissolved in DMSO. Further, a doubling dilution of test JP-AgNPs was performed to achieve concentrations ranging from 0.5 to >64.00 µg/mL whereas, streptomycin and nystatin (0.5 to 15.00 µg/mL). Test JP-AgNPs at various concentrations were then added to culture medium in a 96-well titer plate and different microbial strains were inoculated at 1×10^8 CFU/mL concentration. Muller Hinton broth (MHB) medium was employed for both bacterial and fungal pathogens. The titer plate was incubated at 37 °C for 24 h and then observed for the growth of the tested pathogens. Streptomycin and nystatin were used as standard antibacterial and antifungal drugs, respectively. The lowest concentration of the test JP-AgNPs where the well remained clear, indicating that the bacterial or fungal growth was completely inhibited and that the least concentration was considered as MIC value.

2.6. Characterization

UV-Visible analysis performed on lambda 35, Perkin Elmer, Waltham, MA, USA. Fourier transform infrared analyses were performed on a 1000 FT-IR instrument, Perkin-Elmer Waltham, MA, USA. The FT-IR samples were measured under the resolution of 4 cm^{-1} . The X-ray powder diffraction analysis of the as-prepared silver nanoparticles was performed on D2-Phaser, Bruker, Germany. Transmission electron microscopy (TEM) analysis was performed using JEM-1101, Jeol, Japan. Scanning electron microscopy (SEM) and energy-dispersive X-ray analysis was performed using JSM 7600F instrument, JEOL, Tokyo, Japan. The images were captured under an operational voltage of 5 kV and a working distance of 4.5 mm over different magnifications.

3. Results and Discussions

3.1. UV-Visible Analysis

The silver nanoparticles (JP-AgNPs) formation is monitored by UV-Vis analysis, which is carried out by collecting the reaction mixture from time to time. However, the obvious color transformation in the reaction mixture from light green to dark brown also pointed out the formation of JP-AgNPs. The UV-Vis analysis of the reaction mixture revealed at the start of the reaction, the nucleation process was in progress rapidly, which ensued in the fast development of JP-AgNPs for the first 1 h. After two hours, the nucleation process is found to slow down and no further transformation in the intensity of the absorption

band was noticed, which evidently specified the accomplishment of reaction. The UV–Vis spectrum obtained to display the absorption in the visible range from 370 to 460 nm, with a sharp intense peak appearing at 424 nm (Figure 1a,b) which confirms the formation of JP-AgNPs, additional absorption peaks at 260 nm is also observed, which belongs to the phytomolecules from *J. procera* extract (JP) remaining on the surface of JP-AgNPs as capping agents, which is confirmed by the UV–Vis analysis of an extract of *J. procera* (JP).

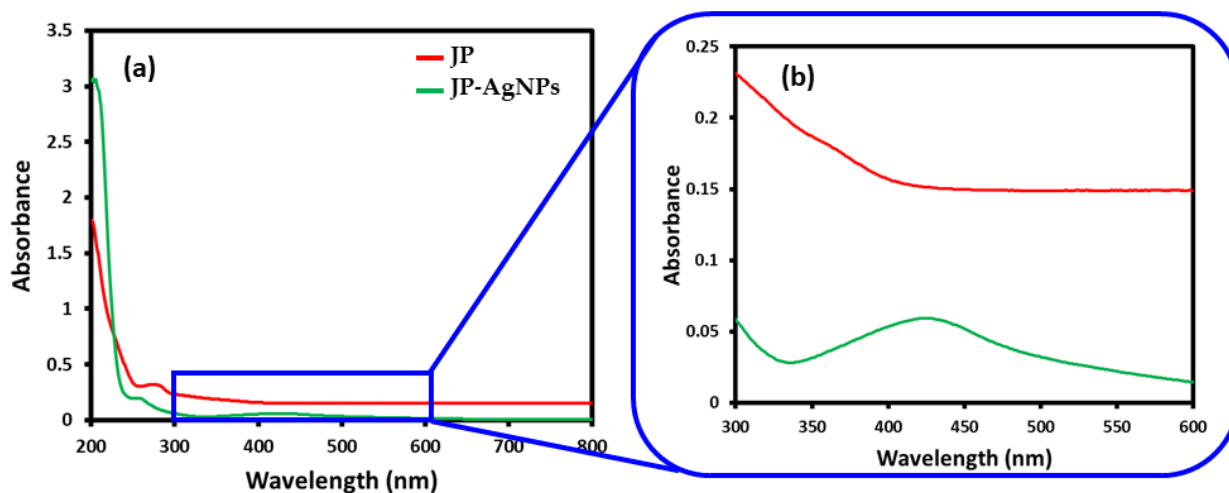


Figure 1. (a) UV–Vis spectra of *J. procera* extract (JP) and as-synthesized silver nanoparticles using *J. procera* extract (JP-AgNPs) and (b) magnified image of Figure 1a.

3.2. XRD Analysis

Figure 2 exhibits the XRD diffraction pattern of silver nanoparticles attained from using *J. procera* extract (JP-AgNPs). The diffractogram pattern of JP-AgNPs exhibited some intense diffractions, which endorses the crystallinity of the as-synthesized JP-AgNPs. The five reflections at 37.70° (111), 44.40° (200), 64.20° (220), 76.90° (311), and 81.33° (222) clearly specified the development of the face-centered cubic (fcc) structure of the JP-AgNPs. Furthermore, the XRD diffraction pattern analysis exhibited some more additional reflections attributed to residual moieties from the *J. procera* extract.

$$d = \frac{n\lambda}{2\sin\theta}$$

$$D = \frac{k\lambda}{\beta\cos\theta}$$

where, a = Lattice Constant, ' d ' is Interplanar Spacing, and h, k, l , = Miller Indices; Debye–Scherrer formula (D).

3.3. FT-IR Analysis

FT-IR analysis was performed to ascertain the possible biomolecules in the *J. procera* extract. FT-IR spectra of plant extract and as-synthesized JP-AgNPs are displayed in Figure 3. The phytomolecules analysis of *J. procera* extract discloses the existence of flavonoids, alkaloids, steroids, rosins, saponins, etc., [24]. In the plant extract, the peaks are noticed at 535, 617, 1063, 1267, 1429, 1603, and 3419 cm^{-1} . After reaction with AgNO_3 , the peaks are shifted slightly, such as 533, 619, 1078, 1273, 1431, 1620, and 3421 cm^{-1} . The strong intense peaks at 1429 cm^{-1} correspond to C–N stretching, which may belong to the proteins in the plant extract [25]. The strong band at 1063 cm^{-1} may correspond to the ether linkages of flavanones [26]. The existing phenolic groups in the plant extract possibly contributing to the reduction are appeared in the ~ 1325 – 1040 and ~ 1455 – 1600 cm^{-1} regions [27]. For example, phenols are typically identified by the characteristic broad band representing OH stretch roughly between 3400 to 3500 cm^{-1} , as appeared in this case at 3410 cm^{-1} . There

is a bend at $\sim 1380\text{ cm}^{-1}$, which may correspond to the O–H bending of both phenol and carboxylic acid. Between the wave numbers 1300 cm^{-1} and 1000 cm^{-1} , the largest peak is at 1247 cm^{-1} and this peak is assigned as the C–O stretch of phenol. Whereas, another sharp peak at 1058 cm^{-1} can be representative of C–O stretching of alcohols. Besides, a sharp band at 1620 cm^{-1} is due to the C=C aromatic ring stretching, pointing towards the existence of the aromatic group. All these peaks strongly indicate the presence of polyphenolic contents in the plant extract. Therefore, the rich polyphenolic and flavonoid contents present in the plant extract can be potentially responsible for reducing and stabilizing the resultant Ag NPs. Indeed, this is further confirmed by an elaborated study on the extraction of extracts from different parts of the *J. procera* plant in a variety of solvents [28]. The study revealed that ethanolic, methanolic extracts of leaves demonstrate high concentrations of total phenolic and total flavonoid content. The majority of these peaks are also existing in the FT-IR spectrum of JP-AgNPs with some marginal shifts. Consequently, the occurrence of these peaks in the FT-IR spectrum of JP-AgNPs is evidently directed towards the effective dual role of the aqueous plant extract of *J. procera*, both as a reducing and stabilizing agent.

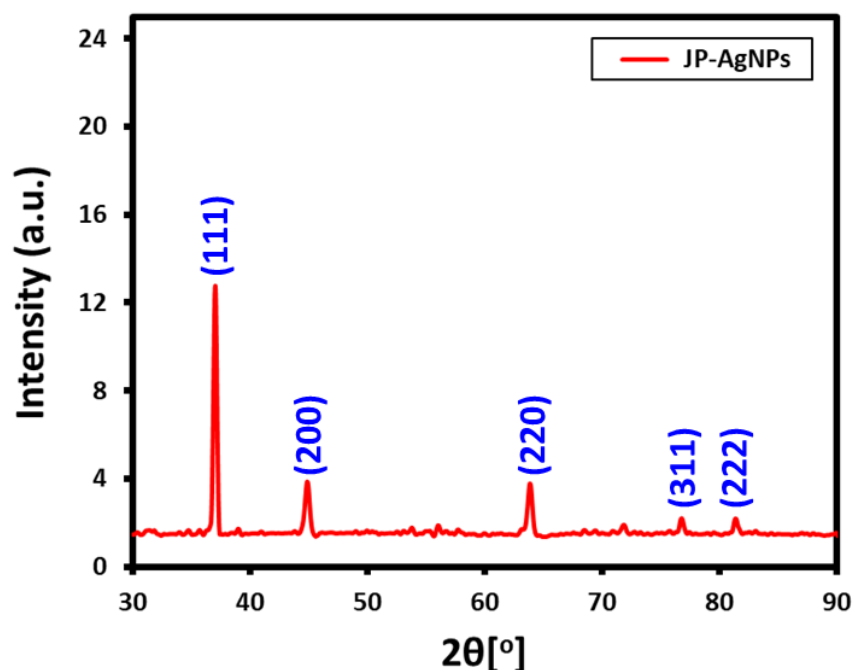


Figure 2. X-ray diffraction (XRD) diffractogram of as-synthesized silver nanoparticles using *J. procera* extract (JP-AgNPs).

The term ' D ' is the Crystal size, ' λ ' corresponds to X-ray wavelength, ' k ' is a dimensionless shape factor, ' β ' is the line broadening at half the maximum intensity, and ' θ ' is Bragg's angle. The average crystallite size of JP-AgNPs is found to be $\sim 23.7\text{ nm}$ (Table 1).

Table 1. XRD results and crystallographic data of the JP-AgNPs.

2θ (°)	FWHM (°)	h, k, l	a (nm)	d (nm)	Crystal Size (D) nm
37.06	0.33	111		0.24	25.12
44.91	0.46	200		0.20	18.84
63.87	0.44	220	0.4106	0.15	21.31
76.76	0.37	311		0.12	27.09
81.36	0.40	222		0.12	26.13

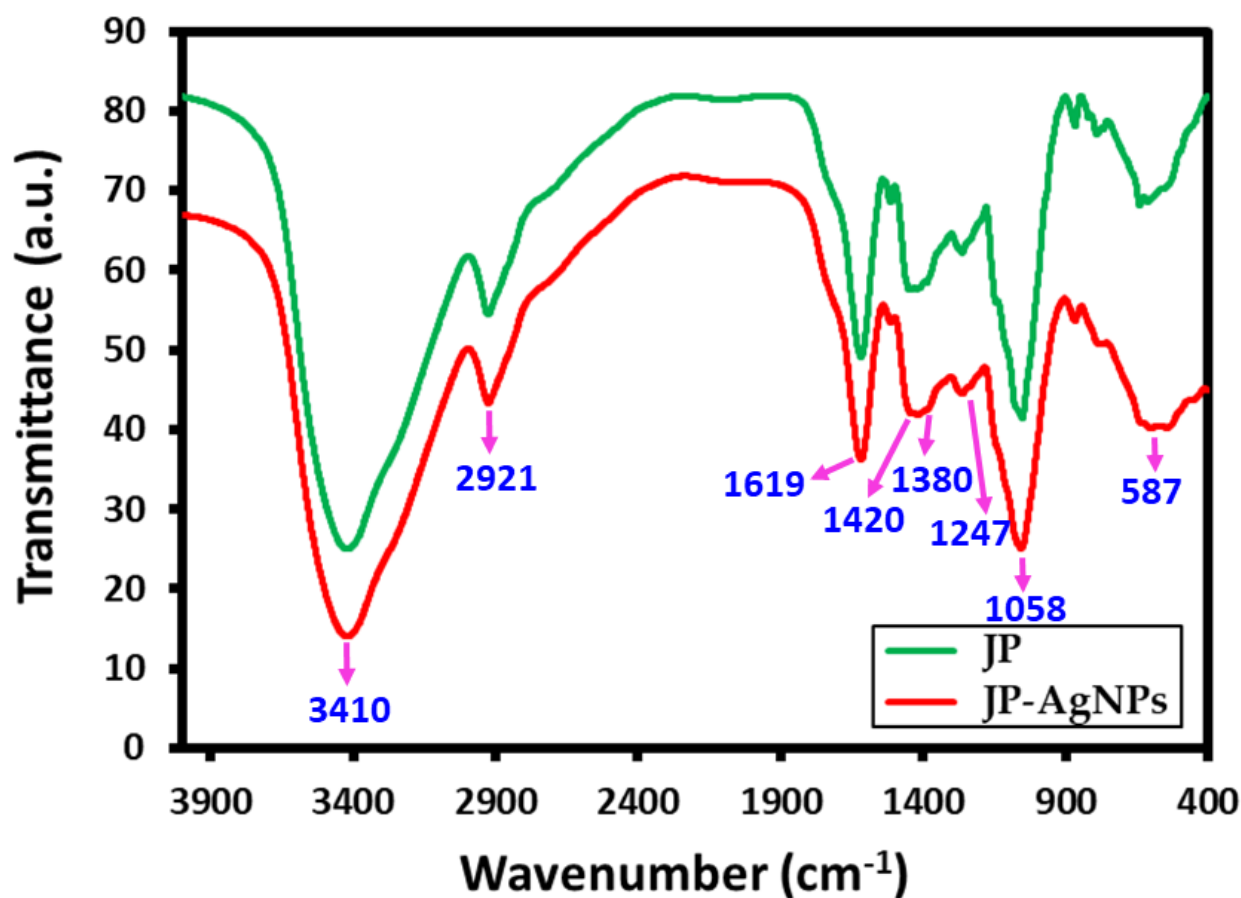


Figure 3. Comparison of the IR spectra of *J. procera* extract and green synthesized silver nanoparticles (JP-AgNPs).

3.4. TEM and EDX Analysis

The as-synthesized size and morphology of JP-AgNPs were investigated by using transmission electron microscopy (TEM) and energy-dispersive X-ray spectroscopy (EDX) analysis (Figure 4). Figure 4a displays the spherical morphology of the JP-AgNPs. The JP-AgNPs are well distributed. Additionally, the particle size distribution graph was estimated by using Image J software (Figure 5), the particle size distribution graph of the JP-AgNPs displays the average particle size is in the range of 10–30 nm. Whereas, in an earlier study, the leaves extract of JP has produced large sized NPs with wide size distribution between 30–90 nm [21]. The relatively high quality of NPs obtained in our study can be due to the presence of large contents of polyphenols and flavonoids in the whole extract of aerial parts of *J. Procera* when compare to the leave extract. Furthermore, Figure 4b exhibits the energy-dispersive X-ray analysis of the synthesized silver nanoparticles, which recommends the existence of silver as the main element. Generally, the silver nanoparticles display a typically strong signal at 3 keV, due to surface plasmon resonance. EDX profile showed a strong signal for silver along with some other signal peaks which might have initiated from the biomolecules that are bound to the surface of JP-AgNPs, representing the reduction of silver ions to elemental silver. The other peak of Cu in the EDX is an artifact of the Cu grid on which the sample was coated. There were no other signal peaks noticed for silver. This authorizes the thorough reduction of silver compounds to JP-AgNPs as revealed in the EDX spectrum.

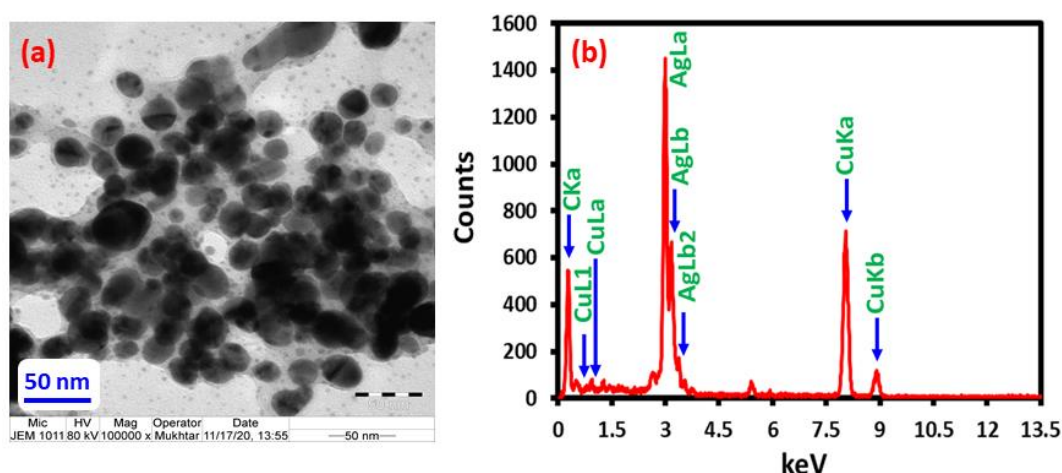


Figure 4. (a) High-resolution transmission electron microscopy (HRTEM) image of the JP-AgNPs and (b) energy-dispersive X-ray spectroscopy (EDX) of JP-AgNPs.

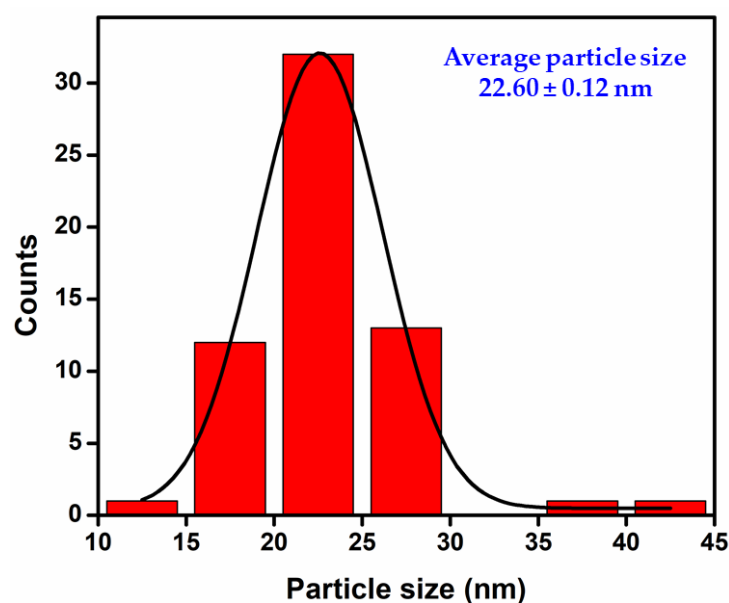


Figure 5. Particle size distribution graph of JP-AgNPs.

3.5. Possible Mechanism of Reduction by Phytomolecules

The antioxidant properties of phytoconstituents consisting of flavonoids, polyphenols are generally caused by their redox properties [29]. Due to this, the polyphenolic compounds function as strong reductants, hydrogen donors, singlet oxygen quenchers [30]. It is believed that these compounds generate reactive hydrogen during the process of tautomerization (conversion from enol-form to the keto-form), which facilitates the reduction of metal ions [31]. Apart from this, other internal oxidations including ketone to carboxylic acid reactions are also known to promote the reduction of metal ions to metal NPs. Therefore, in the case of *J. Procer*, we believe that Ag NPs were probably formed in three different steps similar to the process that occur during polyol based synthesis of NPs [32]. Initially, Ag seeds are generated due to the reduction of metal ions by virtue of the redox properties of polyphenols and flavonoids, this process is referred to as the induction phase. Subsequently, the small Ag seeds ultimately grow into larger aggregates during the growth process. Finally, in the termination phase, the surface of the Ag aggregates are stabilized by the surface-bound phytoconstituents, which also define the final morphology and size of NPs.

3.6. Biological Activity

In the recent past, antimicrobial resistance is a common problem around the globe, more often microbial pathogens are showing resistance against standard drugs in medicine to treat dreadful diseases. However, various chemical and green synthesized nanoparticles are explored in every part of the world and scientific communities extensively investigate the biological potency of such promising nanoparticles. In this lieu, biosynthesized JP-AgNPs were evaluated for their antimicrobial activities.

Overall, these results showed substantial antimicrobial activities against a panel of tested microbial pathogens (Table 2 and Figure 6). The JP-AgNPs exhibited efficient MZI values at 50.00 μ L against bacterial pathogens, especially compared to the fungal pathogens. The MZI range between 8.00 ± 0.28 mm and 17.17 ± 0.72 mm. Particularly, MZI values against microbial pathogens were as follows; *E. coli* (17.17 ± 0.72 mm), *P. mirabilis* (14.80 ± 0.17 mm) and *C. albicans* (14.30 ± 0.60 mm), whereas JP-AgNPs showed moderate activity against *P. aeruginosa* (11.50 ± 0.29 mm) and *C. neoformans* (9.83 ± 0.44 mm). In the case of *S. aureus* (8.00 ± 0.28), it exhibited much less activity compared to all the microbial pathogens. Overall antimicrobial activity of plant extract was moderate when compared with JP-AgNPs, and its range was between 6.50 ± 0.10 and 11.25 ± 0.50 mm. Thus, the tested JP-AgNPs was found to hold as same antimicrobial activities when compared to standard antimicrobial drugs, such as streptomycin and nystatin (Table 2 and Figure 7).

Table 2. Antimicrobial activities of JP-AgNPs against selected microbial pathogens and their significance.

Microbial Pathogens	Mean Zone of Inhibition (MZI) (mm)			Confidence Interval (95%)
	JP Extract [§] (50 μ g) *	JP-AgNPs [#] (50 μ g) *	Streptomycin (10 μ g)	
Gram positive pathogens				
<i>S. aureus</i> ATCC 12228	6.5 ± 0.10	8.0 ± 0.28 ^{b,c,d,e,ns}	20.00	6.76–9.24
Gram negative pathogens				
<i>E. coli</i> ATCC 25922	11.25 ± 0.50	17.17 ± 0.72 ^{a,c,d,e,f}	21.00	14.04–20.29
<i>P. aeruginosa</i> ATCC 27853	9.00 ± 1.00	11.50 ± 0.29 ^{a,b,d,e,ns}	17.00	10.26–12.74
<i>P. mirabilis</i> ATCC 4753	8.75 ± 1.25	14.80 ± 0.17 ^{a,b,c,ns,f}	19.00	14.12–15.55
Fungal pathogens				
<i>C. albicans</i> ATCC 885653	10.15 ± 0.75	14.30 ± 0.60 ^{a,b,c,ns,f}	18.00	11.75–16.92
<i>C. neoformans</i> ATCC 16620	9.50 ± 0.25	9.80 ± 0.44 ^{ns,b,ns,d,e}	16.00	7.93–11.73

^{#a.} significant at the level of $p < 0.05$ in comparison with *S. aureus*; ^{b.} significant at the level of $p < 0.05$ in comparison with *E. coli*; ^{c.} significant at the level of $p < 0.05$ in comparison with *P. aeruginosa*; ^{d.} significant at the level of $p < 0.05$ in comparison with *P. mirabilis*; ^{e.} significant at the level of $p < 0.05$ in comparison with *C. albicans*; ^{f.} significant at the level of $p < 0.05$ in comparison with *C. neoformans*; ^{ns}—non-significant; [§]—statistically non-significant; * = 50 μ L of the solution from the stock solution of 1 mg/mL was used, which is equivalent to 50 μ g of the powder.

In addition, the assessment of prospective antimicrobials was determined by MIC for the JP-AgNPs with MZI values above or equal to 12.00 mm. The results displayed in Table 3, showed that the tested JP-AgNPs possessed significant antimicrobial activities with minimum (16.00 μ g/mL) and maximum (>64.00 μ g/mL) MIC value. The JP-AgNPs showed a significant MIC value against *E. coli* and *C. albicans* (16.00 μ g/mL) followed by *P. mirabilis* and *P. aeruginosa* (32.00 μ g/mL). This antimicrobial activity incident was described among different strains variation and JP-AgNPs stabilization. Comparatively, MIC values of tested JP-AgNPs were moderately lower than commercially available antimicrobial drugs tested in this study. However, enhanced antimicrobial activity of JP-AgNPs due to synthesis with uniform shape, size, and particle size distribution and also colloidal stability of nanoparticles interacted with the cell wall of microbial pathogens [33,34].

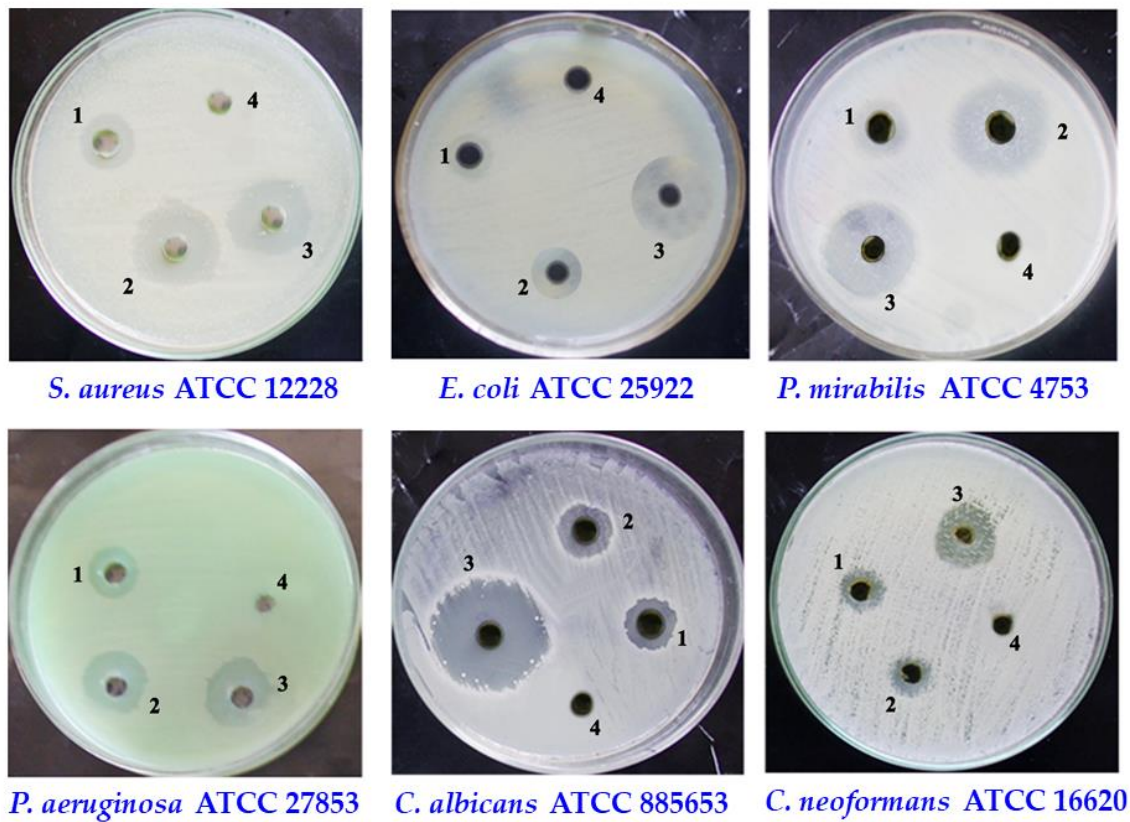


Figure 6. Biological activity of JP extract, JP-AgNPs against various bacterial and fungal strains (1. JP extract, 2. JP-AgNPs, 3. Streptomycin, and 4. DMSO).

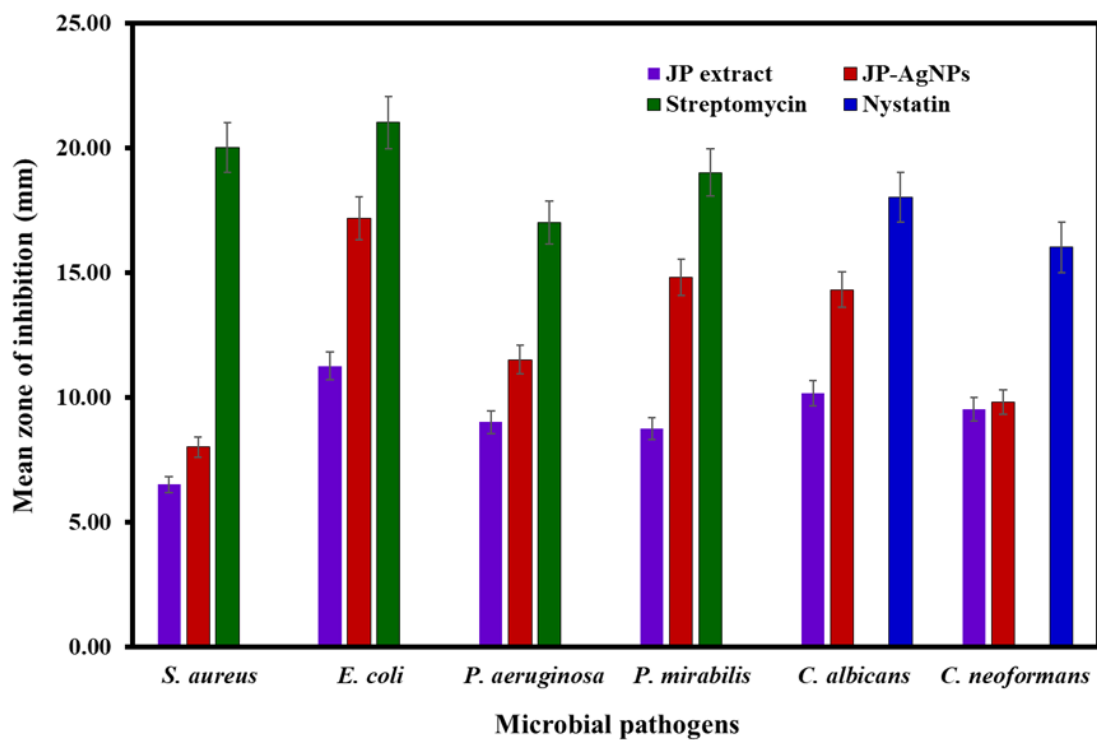


Figure 7. Antimicrobial efficiency of pure JP extract, JP-AgNPs streptomycin (antibacterial drug) and nystatin (antifungal drug) against microbial pathogens by mean zone of inhibition.

Table 3. MIC values of JP-AgNPs against selected microbial pathogens.

Microbial Pathogens	MIC Value ($\mu\text{g/mL}$)	
	Streptomycin	JP-AgNPs
Gram-positive pathogen		
<i>S. aureus</i> ATCC 12228	10.00	>64.00
Gram-negative pathogens		
<i>E. coli</i> ATCC 25922	5.00	16.00
<i>P. aeruginosa</i> ATCC 27853	5.00	32.00
<i>P. mirabilis</i> ATCC 4753	5.00	32.00
Fungal pathogens		Nystatin
<i>C. albicans</i> ATCC 885653	5.00	16.00
<i>C. neoformans</i> ATCC 16620	10.00	64.00

It is widely believed that the antimicrobial activity of nanoparticles usually occur due to the breaking of cell walls, and leakages in the cell membranes [35]. In this case, also the JP-AgNPs were possibly clinging to the bacteria cell wall and liberated silver ions into the bacteria cell by the process of diffusion, which ultimately disrupts the cell wall and causes the death of the bacteria.

In addition, this massive antimicrobial activity is mainly due to the formation of reactive oxygen species (ROS) inside the pathogens [22]. Moreover, the development of the electron spin effect by JP-AgNPs drives the accumulation of free radicals. The free radicals readily interact with the cell membrane of pathogens and create pores resulting in the death of microbial pathogens [36,37]. Reports also demonstrate that JP-AgNPs disrupt the cellular metabolism by which control DNA replication and ATP synthesis [38].

4. Conclusions

In the present study, a novel approach for the synthesis of silver nanoparticles from *J. procera* plant extract was given. The as-synthesized JP-AgNPs are characterized by various characterization techniques such as UV–Vis, XRD, FT-IR, TEM, and EDX analysis. The as-synthesized JP-AgNPs were spherically shaped with the size of ~20 nm. The UV–Vis spectral analysis confirmed the formation of JP-AgNPs. Potential biomolecules responsible for reducing and stabilizing the silver nanoparticles are indicated by FT-IR measurements. Furthermore, the synthesized JP-AgNPs were evaluated for antibacterial properties against several bacterial and fungal strains such as *S. aureus* (ATCC 12228), *E. coli* (ATCC 25922), *P. aeruginosa* (ATCC 27853), *P. mirabilis* (ATCC 4753), *C. neoformans* (ATCC 16620), and *C. albicans* (ATCC 885-653). The tested JP-AgNPs were found to possess almost similar antimicrobial activities to that of standard antimicrobial drugs, such as streptomycin and nystatin. The JP-AgNPs have revealed antibacterial against a wide range of pathogenic bacteria which recognized their application in biomedicine. Furthermore, it is concluded that the synthesis of AgNPs using *J. procera* extract is an inexpensive, easy and eco-friendly approach that eliminates the application of toxic reagents which may cause environmental damage.

Author Contributions: Conceptualization, M.K. (Merajuddin Khan), M.R.S. and M.K. (Mujeeb Khan); methodology, M.K. (Merajuddin Khan), M.R.S. and M.K. (Mujeeb Khan); validation, S.F.A.; formal analysis, P.K., H.Z.A., M.K. (Mufsir Kuniyil) and S.F.A.; investigation, M.R.S.; resources, M.K. (Merajuddin Khan) and S.F.A.; data curation, M.K. (Mufsir Kuniyil) and M.R.S.; writing—original draft preparation, M.K. (Merajuddin Khan) and M.R.S.; writing—review and editing, M.K. (Mujeeb Khan); visualization, M.R.S.; supervision, S.F.A. and M.K. (Merajuddin Khan); project administration, M.K. (Merajuddin Khan); funding acquisition, M.K. (Merajuddin Khan). All authors have read and agreed to the published version of the manuscript.

Funding: The authors extend their appreciation to the Deputyship for Research & Innovation, Ministry of Education in Saudi Arabia for funding this research work through the project number (DRI-KSU-1306).

Institutional Review Board Statement: Not applicable.

Informed Consent Statement: Not applicable.

Data Availability Statement: Data contained within the article.

Acknowledgments: The authors extend their appreciation to the Deputyship for Research & Innovation, Ministry of Education in Saudi Arabia for funding this research work through the project number (DRI-KSU-1306).

Conflicts of Interest: The authors declare no conflict of interest.

References

1. Guerra, F.D.; Attia, M.F.; Whitehead, D.C.; Alexis, F. Nanotechnology for Environmental Remediation: Materials and Applications. *Molecules* **2018**, *23*, 1760. [[CrossRef](#)] [[PubMed](#)]
2. Singh, A.; Dubey, S.; Dubey, H.K. Nanotechnology: The future engineering. *Nanotechnology* **2019**, *6*, 230–233.
3. Gordon, R.; Losic, D.; Tiffany, M.A.; Nagy, S.S.; Sterrenburg, F.A. The Glass Menagerie: Diatoms for novel applications in nanotechnology. *Trends Biotechnol.* **2009**, *27*, 116–127. [[CrossRef](#)]
4. Whitesides, G.M. Nanoscience, nanotechnology, and chemistry. *Small* **2005**, *1*, 172–179. [[CrossRef](#)]
5. Bayda, S.; Adeel, M.; Tuccinardi, T.; Cordani, M.; Rizzolio, F. The History of Nanoscience and Nanotechnology: From Chemical-Physical Applications to Nanomedicine. *Molecules* **2020**, *25*, 112. [[CrossRef](#)]
6. Pareek, V.; Gupta, R.; Panwar, J. Do physico-chemical properties of silver nanoparticles decide their interaction with biological media and bactericidal action? A review. *Mater. Sci. Eng. C* **2018**, *90*, 739–749. [[CrossRef](#)] [[PubMed](#)]
7. Shaik, M.R.; Albalawi, G.H.; Khan, S.; Khan, M.; Adil, S.F.; Kuniyil, M.; Al-Warthan, A.; Siddiqui, M.R.H.; Alkhatlan, H.Z.; Khan, M. “Miswak” Based Green Synthesis of Silver Nanoparticles: Evaluation and Comparison of Their Microbicidal Activities with the Chemical Synthesis. *Molecules* **2016**, *21*, 1478. [[CrossRef](#)] [[PubMed](#)]
8. Khan, M.; Al-Hamoud, K.; Liaqat, Z.; Shaik, M.R.; Adil, S.F.; Kuniyil, M.; Alkhatlan, H.Z.; Al-Warthan, A.; Siddiqui, M.R.H.; Mondeshki, M.; et al. Synthesis of Au, Ag, and Au-Ag Bimetallic Nanoparticles Using *Pulicaria undulata* Extract and Their Catalytic Activity for the Reduction of 4-Nitrophenol. *Nanomaterials* **2020**, *10*, 1885. [[CrossRef](#)]
9. Riaz, M.; Suleman, A.; Ahmad, P.; Khandaker, M.U.; Alqahtani, A.; Bradley, D.A.; Khan, M.Q. Biogenic Synthesis of AgNPs Using Aqueous Bark Extract of *Aesculus indica* for Antioxidant and Antimicrobial Applications. *Crystals* **2022**, *12*, 252. [[CrossRef](#)]
10. Chinni, S.; Gopinath, S.; Anbu, P.; Fuloria, N.; Fuloria, S.; Mariappan, P.; Krusnamurthy, K.; Reddy, L.V.; Ramachawolran, G.; Sreeramanan, S.; et al. Characterization and Antibacterial Response of Silver Nanoparticles Biosynthesized Using an Ethanolic Extract of *Coccinia indica* Leaves. *Crystals* **2021**, *11*, 97. [[CrossRef](#)]
11. Nazneen, H.; Rather, G.A.; Ali, A.; Chakravorty, A. The Role of Plant-Mediated Biosynthesized Nanoparticles in Agriculture. In *Sustainable Agriculture*; Springer: Berlin/Heidelberg, Germany, 2022; pp. 97–117. [[CrossRef](#)]
12. Al-Yousef, H.M.; Amina, M.; Alqahtani, A.S.; Alqahtani, M.S.; Malik, A.; Hatshan, M.R.; Siddiqui, M.R.H.; Khan, M.; Shaik, M.R.; Ola, M.S.; et al. Pollen Bee Aqueous Extract-Based Synthesis of Silver Nanoparticles and Evaluation of Their Anti-Cancer and Anti-Bacterial Activities. *Processes* **2020**, *8*, 524. [[CrossRef](#)]
13. Shaik, M.R.; Ali, Z.J.Q.; Khan, M.; Kuniyil, M.; Assal, M.E.; Alkhatlan, H.Z.; Al-Warthan, A.; Siddiqui, M.R.H.; Khan, M.; Adil, S.F. Green Synthesis and Characterization of Palladium Nanoparticles Using *Origanum vulgare* L. Extract and Their Catalytic Activity. *Molecules* **2017**, *22*, 165. [[CrossRef](#)]
14. Yi, Y.; Wang, C.; Cheng, X.; Yi, K.; Huang, W.; Yu, H. Biosynthesis of Silver Nanoparticles by *Conyza canadensis* and Their Antifungal Activity against *Bipolaris maydis*. *Crystals* **2021**, *11*, 1443. [[CrossRef](#)]
15. Al-Hamoud, K.; Shaik, M.R.; Khan, M.; Alkhatlan, H.Z.; Adil, S.F.; Kuniyil, M.; Assal, M.E.; Al-Warthan, A.; Siddiqui, M.R.H.; Tahir, M.N.; et al. *Pulicaria undulata* Extract-Mediated Eco-Friendly Preparation of TiO₂ Nanoparticles for Photocatalytic Degradation of Methylene Blue and Methyl Orange. *ACS Omega* **2022**, *7*, 4812–4820. [[CrossRef](#)] [[PubMed](#)]
16. Lohithan, R.; Raj, R.; Prakash, P.; Santosh, A.; Theertha, V.; Chandran, S. Green synthesis of silver nanoparticles from *Justicia adhatodaplant* extract with its diverse properties. *J. Phys. Conf. Ser.* **2020**, *1706*, 012012. [[CrossRef](#)]
17. Hussain, I.; Singh, N.B.; Singh, A.; Singh, H.; Singh, S.C. Green synthesis of nanoparticles and its potential application. *Biotechnol. Lett.* **2016**, *38*, 545–560. [[CrossRef](#)] [[PubMed](#)]
18. Sharifi-Rad, M.; Pohl, P.; Epifano, F.; Álvarez-Suarez, J.M. Green synthesis of silver nanoparticles using *Astragalus tribuloides delile*. root extract: Characterization, antioxidant, antibacterial, and anti-inflammatory activities. *Nanomaterials* **2020**, *10*, 2383. [[CrossRef](#)]
19. Singh, R.; Hano, C.; Nath, G.; Sharma, B. Green biosynthesis of silver nanoparticles using leaf extract of *Carissa carandas* L. and their antioxidant and antimicrobial activity against human pathogenic bacteria. *Biomolecules* **2021**, *11*, 299. [[CrossRef](#)] [[PubMed](#)]

20. Abdelghany, T.; Hassan, M.M.; El-Naggar, M.A.; El-Mongy, M.A. GC/MS analysis of Juniperus procera extract and its activity with silver nanoparticles against Aspergillus flavus growth and aflatoxins production. *Biotechnol. Rep.* **2020**, *27*, e00496. [[CrossRef](#)] [[PubMed](#)]
21. Ibrahim, E.; Kilany, M.; Ghramh, H.A.; Khan, K.; Islam, S.U. Cellular proliferation/cytotoxicity and antimicrobial potentials of green synthesized silver nanoparticles (AgNPs) using Juniperus procera. *Saudi J. Biol. Sci.* **2019**, *26*, 1689–1694. [[CrossRef](#)] [[PubMed](#)]
22. Morones, J.R.; Elechiguerra, J.L.; Camacho, A.; Holt, K.; Kouri, J.B.; Ramírez, J.T.; Yacaman, M.J. The bactericidal effect of silver nanoparticles. *Nanotechnology* **2005**, *16*, 2346–2353. [[CrossRef](#)]
23. Wayne, P. Clinical and laboratory standards institute. Performance standards for antimicrobial susceptibility testing. *CLSI Doc. M100-S20* **2011**, *31*, 100–121.
24. Rajashekar, V.; Rao, E.U.; Srinivas, P. Biological activities and medicinal properties of Gokhru (*Pedalium murex* L.). *Asian Pac. J. Trop. Biomed.* **2012**, *2*, 581–585. [[CrossRef](#)]
25. Gurunathan, S.; Jeong, J.-K.; Han, J.W.; Zhang, X.-F.; Park, J.H.; Kim, J.-H. Multidimensional effects of biologically synthesized silver nanoparticles in Helicobacter pylori, Helicobacter felis, and human lung (L132) and lung carcinoma A549 cells. *Nanoscale Res. Lett.* **2015**, *10*, 35. [[CrossRef](#)] [[PubMed](#)]
26. Shankar, S.S.; Rai, A.; Ahmad, A.; Sastry, M. Rapid synthesis of Au, Ag, and bimetallic Au core-Ag shell nanoparticles using Neem (*Azadirachta indica*) leaf broth. *J. Colloid Interface Sci.* **2004**, *275*, 496–502. [[CrossRef](#)]
27. Jeeva, K.; Thiagarajan, M.; Elangovan, V.; Geetha, N.; Venkatachalam, P. Caesalpinia coriaria leaf extracts mediated biosynthesis of metallic silver nanoparticles and their antibacterial activity against clinically isolated pathogens. *Ind. Crops Prod.* **2014**, *52*, 714–720. [[CrossRef](#)]
28. Salih, A.M.; Al-Qurainy, F.; Nadeem, M.; Tarrour, M.; Khan, S.; Shaikhaldein, H.O.; Al-Hashimi, A.; Alfagham, A.; Alkahtani, J. Optimization Method for Phenolic Compounds Extraction from Medicinal Plant (*Juniperus procera*) and Phytochemicals Screening. *Molecules* **2021**, *26*, 7454. [[CrossRef](#)] [[PubMed](#)]
29. Cotellet, N.; Hapiot, P.; Pinson, J.; Rolando, A.C.; Vezin, H. Polyphenols Deriving from Chalcones: Investigations of Redox Activities. *J. Phys. Chem. B* **2005**, *109*, 23720–23729. [[CrossRef](#)]
30. Rice-Evans, C.A.; Miller, N.J.; Bolwell, P.G.; Bramley, P.M.; Pridham, J.B. The Relative Antioxidant Activities of Plant-Derived Polyphenolic Flavonoids. *Free Radic. Res.* **1995**, *22*, 375–383. [[CrossRef](#)] [[PubMed](#)]
31. Makarov, V.; Love, A.; Sinityna, O.; Makarova, S.; Yaminsky, I.; Taliansky, M.; Kalinina, N. “Green” nanotechnologies: Synthesis of metal nanoparticles using plants. *Acta Nat.* **2014**, *6*, 35–43. [[CrossRef](#)]
32. Khan, M.; Shaik, M.R.; Adil, S.F.; Khan, S.T.; Al-Warthan, A.; Siddiqui, M.R.H.; Tahir, M.N.; Tremel, W. Plant extracts as green reductants for the synthesis of silver nanoparticles: Lessons from chemical synthesis. *Dalton Trans.* **2018**, *47*, 11988–12010. [[CrossRef](#)]
33. Melaiye, A.; Sun, Z.; Hindi, K.; Milsted, A.; Ely, D.; Reneker, D.H.; Tessier, C.A.; Youngs, W.J. Silver(I)–Imidazole Cyclophane gem-Diol Complexes Encapsulated by Electrospun Tecophilic Nanofibers: Formation of Nanosilver Particles and Antimicrobial Activity. *J. Am. Chem. Soc.* **2005**, *127*, 2285–2291. [[CrossRef](#)] [[PubMed](#)]
34. Chudasama, B.; Vala, A.K.; Andhariya, N.; Mehta, R.V.; Upadhyay, R.V. Highly bacterial resistant silver nanoparticles: Synthesis and antibacterial activities. *J. Nanoparticle Res.* **2010**, *12*, 1677–1685. [[CrossRef](#)]
35. Li, W.-R.; Xie, X.-B.; Shi, Q.-S.; Zeng, H.-Y.; Ou-Yang, Y.-S.; Chen, Y.-B. Antibacterial activity and mechanism of silver nanoparticles on *Escherichia coli*. *Appl. Microbiol. Biotechnol.* **2010**, *85*, 1115–1122. [[CrossRef](#)] [[PubMed](#)]
36. Danilczuk, M.; Lund, A.; Sadlo, J.; Yamada, H.; Michalik, J. Conduction electron spin resonance of small silver particles. *Spectrochim. Acta Part A Mol. Biomol. Spectrosc.* **2006**, *63*, 189–191. [[CrossRef](#)]
37. Kim, J.S.; Kuk, E.; Yu, K.N.; Kim, J.-H.; Park, S.J.; Lee, H.J.; Kim, S.H.; Park, Y.K.; Park, Y.H.; Hwang, C.-Y.; et al. Antimicrobial effects of silver nanoparticles. *Nanomed. Nanotechnol. Boil. Med.* **2007**, *3*, 95–101, Erratum in *Nanomed. Nanotechnol. Biol. Med.* **2014**, *10*, e1119. [[CrossRef](#)] [[PubMed](#)]
38. Marambio-Jones, C.; Hoek, E.M.V. A review of the antibacterial effects of silver nanomaterials and potential implications for human health and the environment. *J. Nanopart. Res.* **2010**, *12*, 1531–1551. [[CrossRef](#)]